

Properties of threading screw dislocation core in wurtzite GaN studied by Heyd-Scuseria-Ernzerhof hybrid functional

M. Matsubara,¹ J. Godet,² L. Pizzagalli,² and E. Bellotti¹

¹*ECE, Boston University, 8 Saint Mary's Street, Boston, Massachusetts 02215, USA*

²*Institut P', CNRS UPR 3346, Université de Poitiers, SP2MI, BP 30179, Boulevard Marie et Pierre Curie, 86962 Futuroscope Chasseneuil Cedex, France*

(Received 20 September 2013; accepted 13 December 2013; published online 30 December 2013)

We propose another structure as the most stable configuration for threading screw dislocation core of wurtzite GaN in N-rich conditions by first-principles calculations using Heyd-Scuseria-Ernzerhof hybrid functional. This configuration is fully consistent with recent experimental results observing electrical inactivity of GaN samples grown in N-rich conditions, in contrast with previously suggested dislocation core structures. © 2013 AIP Publishing LLC.

[<http://dx.doi.org/10.1063/1.4858618>]

The III-nitrides are important and promising materials for opto- and power electronic device applications. However, the high density of threading dislocations limits the device performance by reducing the carrier mobilities^{1,2} and by introducing deep states in the band gap acting as non-radiative recombination centers³ and could lead to premature device breakdown. Threading dislocations in wurtzite III-nitrides are originated from the mismatched interface between substrates and are aligned along the [0001] direction. Their Burgers vectors (Bvs) are $\langle 11\bar{2}0 \rangle / 3$ (edge), $\langle 0001 \rangle$ (screw), or $\langle 11\bar{2}3 \rangle / 3$ (mixed). In case of wurtzite GaN, screw dislocations are found to be main sources of reverse bias current leakage.⁴ Thus, they have large impact on electronic properties of GaN and related materials. The reverse bias current leakage results are obtained for the samples grown under Ga-rich conditions, because the growth of GaN samples by molecular beam epitaxy has been normally done under Ga-rich conditions to obtain smooth surface morphologies. Recently, significant progress is made in growth technique⁵ and low surface roughness samples grown under N-rich conditions are reported. In these samples, the reverse bias leakage is absent despite the observation of consistent densities of threading screw dislocations with open core type nanopipe structures.⁶ This experimental result is in contrast with the previous theoretical models, which are expected to be electrically active due to induced gap states.^{7,8} In this work, we propose another structure as the most stable screw dislocation core on the basis of state-of-the-art hybrid density functional calculations, which is in agreement with the experimentally observed electrical inactivity in N-rich conditions.

So far, several types of core structures have been proposed for threading screw dislocations in wurtzite GaN. However, the question, which one among them is energetically the most stable, is still subjected to controversy. Traditionally, in theoretical models, the dislocation line is supposed to be positioned at the center of a projected hexagon onto the basal plane, as shown in Fig. 1. We will call it the screw “A” core by analogy with the case of c-Si.^{9–11} Based on this screw “A” core, stoichiometric full core and open core¹² as well as non-stoichiometric core structures^{7,13}

have been proposed. For stoichiometric “A” core structures, Elsner *et al.*¹² have shown that, using density functional theory (DFT) calculations within the local density approximation (LDA), the open core structure is more stable than the full core structure. Subsequently, Northrup has predicted, once again using DFT LDA-based calculation, that non-stoichiometric “A” core structures (Ga-filled core structure, denoted by (6:0) in Ref. 7, in Ga-rich conditions and N-half-removed core structure, denoted by (6:3), in N-rich conditions) are more stable than stoichiometric full or open core structures.^{7,13} Both core structures have been shown to induce dislocation states deep inside the gap. Therefore, threading screw dislocations are expected to be electrically active regardless of sample growth conditions.⁷ Belabbas *et al.*⁸ recently studied another threading screw dislocation type with full core structure, whose formation energy is lower than the screw “A” open core structure. In this structure, which was originally proposed by Béré and Serra,¹⁴ the dislocation line is positioned at the middle of the bond connecting two adjacent projected hexagons, as indicated by the letter B in Fig. 1.

In this Letter, we have investigated the energetics of all previously proposed models, the four “A” cores (full, open, Ga-filled, and N-half-removed) and one “B” core (full) mentioned above using state-of-the-art hybrid density functional, and three more structures based on “B” core, which have open, Ga-filled, and N-half-removed configurations. The latter are obtained by removing all Ga and N atoms (open), all of the N atoms (Ga-filled) and half of the N atoms (N-half-removed) within an ~ 2 Å radius of the dislocation line (open core type structure is shown in Fig. 2). The band structures along the dislocation direction have also been computed for the most stable structures, and their electronic properties are discussed.

To perform this analysis, we employ a first-principles method using hybrid Hartree-Fock density functionals. Hybrid functionals provide an effective method to overcome the so called “band-gap problem”: specifically, the underestimation of the Kohn-Sham energy gap that is encountered when employing LDA or generalized gradient approximation (GGA). In recent years, a growing number of investigations

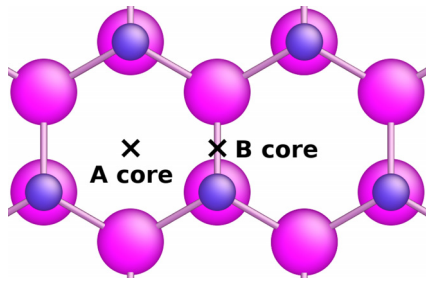


FIG. 1. Two different positions of threading screw dislocation projected onto the (0001) plane. The “A” core is located at the center of projected hexagon, while the “B” core at the middle of the bond connecting two adjacent hexagons.

concerning the electronic structure of defects in semiconductors have been addressed employing hybrid functionals, leading to improved results compared to LDA and GGA.^{20–23} In this work, we employ the Heyd-Scuseria-Ernzerhof (HSE) hybrid functional²⁴ that has been shown to be reliable in predicting a variety of semiconductor bulk material parameters²⁵ and also to give a relatively good surface gap value among common hybrid functionals.²⁶

The calculations performed in this work were carried out using the projector augmented wave method²⁷ with both the Perdew-Burke-Ernzerhof (PBE) GGA functional²⁸ and HSE hybrid functional implemented in the VASP code.²⁹ In the HSE calculation, the amount of exact exchange was set to 28%, leading to a band gap value of 3.45 eV, which is very close to the experimental value for bulk GaN. The Ga 3*d* electrons were treated as valence electrons and the energy cutoff was set to 425 eV. It is already shown that treating the semicore Ga 3*d* electrons as valence electrons increases the accuracy of the formation energy.⁷ Fully periodic oblique (non-orthorhombic) supercell including a dislocation dipole, whose directions of Burgers vectors are opposite each other, is employed. This geometry is obtained by placing the dislocations of the quadrupole in a symmetric way.^{30,31} The three vectors, which define our supercell, are $c_1 = 8a\hat{x}$, $c_2 = 4a\hat{x} + 2\sqrt{3}a\hat{y} + 0.5c\hat{z}$ and $c_3 = c\hat{z}$, where a and c are optimized lattice constants of GaN. Up to 128 atoms are included in this supercell. The Brillouin-zone integration has been performed with three irreducible k points along c direction, which is sufficient to obtain converged energies.

In order to check the convergence of relative formation energies against the cell size, we performed a series of empirical potential calculations using a GaN Stillinger-Weber potential.³² We found that the differences in energy values

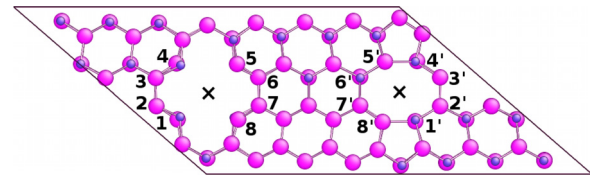


FIG. 2. The “B” open core structure projected onto the (0001) plane. The positions of the dislocation lines are denoted by cross. Fully relaxed structure by calculation within HSE is shown.

between our cell including up to 128 atoms and a larger cell including up to 1152 atoms are less than 0.2 eV for different dislocation core structures.

In Table I, we list basic properties of bulk GaN including lattice constant, energy gap, heat of formation, bulk modulus, and elastic constants by both HSE and PBE. Based on these lattice parameters, initial screw dislocation core configurations have been generated using elasticity theory.³³ We have considered the following eight core structures: full, open, Ga-filled, and N-half-removed cores for both screw “A” and “B” types. For all these core structures, we performed total energy calculations using both HSE and PBE.

The formation energy is evaluated as

$$E^f = E_{tot} - n_{\text{Ga}}\mu_{\text{Ga}} - n_{\text{N}}\mu_{\text{N}}. \quad (1)$$

Here, E_{tot} is the total energy with dislocation, n_{Ga} (n_{N}) is the number of Ga (N) atoms in the supercell with its chemical potential μ_{Ga} (μ_{N}). These chemical potentials must satisfy the following thermodynamic stability condition:

$$\mu_{\text{Ga}} + \mu_{\text{N}} = E(\text{GaN}) = E(\text{Ga}) + \frac{1}{2}E(\text{N}_2) + \Delta H_f(\text{GaN}), \quad (2)$$

where $E(\text{GaN})$, $E(\text{Ga})$, $E(\text{N}_2)$, and $\Delta H_f(\text{GaN})$ denote the energies for bulk GaN, bulk Ga, N_2 molecule, and heat of formation for GaN, respectively. With this constraint the formation energies are expressed as a function of the gallium chemical potential only. In Ga-rich conditions, $\mu_{\text{Ga}} = E(\text{Ga})$, whereas in N-rich conditions $\mu_{\text{Ga}} = E(\text{Ga}) + \Delta H_f(\text{GaN})$.

In order to evaluate the relative stabilities of different core structures, the formation energies for all the core structures obtained by PBE and HSE are plotted relative to the energy of “A” full core structure in Figs. 3(a) and 3(b), respectively. PBE and HSE results are quite similar; in both cases, only three types of core structures are important. In Ga-rich conditions, the “A” Ga-filled core (Figs. 3(a) and 3(b)) is the most

TABLE I. Computed and experimental reference lattice constants (a , c and u), energy gap (in eV), heat of formation (in eV), bulk modulus (in GPa), and elastic constants (in GPa).

	a (Å)	c (Å)	u	E_{gap}	ΔH_f	B_0	C_{11}	C_{12}	C_{13}	C_{33}	C_{44}
PBE	3.219	5.245	0.377	1.71	−0.90	169	322	111	77	356	89
HSE	3.178	5.171	0.377	3.45	−1.18	199	371	133	95	407	102
Expt	3.190 ^a	5.189 ^a	0.375 ^a	3.50 ^b	−1.63 ^c −1.14 ^d	210 ^e	390 ^e	145 ^e	106 ^e	398 ^e	105 ^e

^aReference 15.

^bReference 16.

^cReference 17.

^dReference 18.

^eReference 19.

stable. This is consistent with Northrup's⁷ result obtained within the LDA. In N-rich conditions, the "B" open core is the most stable model (Figs. 3(a) and 3(b)). Previously suggested "A" N-half-removed core⁷ and "B" full core⁸ exhibit much higher formation energies in N-rich conditions. The new "B" Ga-filled core is also favored in the intermediate range of chemical potential, whereas the "B" N-half-removed core is never favorable. We now describe these stable cores using HSE results. Although the relative formation energies obtained by PBE and HSE are quite similar, one of the main reasons we adopt the HSE results is that the band gap value obtained by HSE is very close to the experimental one (see Table I). Therefore, we can evaluate the electronic structure (shown later) precisely without resorting to the artificial band gap correction procedure. In the "A" Ga-filled core configuration, Ga atoms inside the core region (six per Bv) have two bonds with other Ga atoms inside the core: one shorter bond (an average value of 2.50 Å) and one longer bond (an average value of 2.66 Å). They also have one bond with N atoms outside core region with an average bond length of 1.98 Å. The average bond angle value, 107°, is very close to the ideal value (109°) of four-fold coordinated three-dimensional sp^3 bonding. As a result, these Ga atoms inside the core region have one dangling bond.

Figure 4(a) presents the energy band structure along the [0001] direction for the "A" Ga-filled core. Twelve states are

introduced into the bulk band gap (defined by the two dashed red lines, which correspond to conduction band minimum and valence band maximum of bulk, respectively). Half of these 12 states are filled (below Fermi energy, located at 0 eV) while the other half are empty states (above Fermi energy). These states are originated from Ga dangling bonds along the dislocation lines. Indeed, the characterization of these twelve states by wavefunction projection onto atomic orbitals shows that all these states mainly have the Ga 4*p* character. It can be immediately appreciated that, compared to the bulk GaN, the band gap is significantly narrowed by these newly introduced gap states, which are extremely dispersive. This result is consistent with previous LDA calculation.⁷

For "B" open core configuration, two different types of core structures are obtained. One has a hollow core structure as shown in the left part of Fig. 2. The other has an eight-membered ring with two adjacent five-membered rings, as presented in the right part of Fig. 2. These two configurations have very close core energies, less than ≈ 0.2 eV/Bv, therefore it is likely that they could co-exist, especially at high temperature. In the hollow core structure, both Ga and N atoms at the sites denoted by 1, 4, 5, and 8 (i.e., nearest sites to the dislocation line) in Fig. 2 are three-fold coordinated, while those at 2, 3, 6, and 7 sites are four-fold coordinated. The bond lengths and angles are reported in Table II. The three-fold coordinated Ga (N) atoms adopt sp^2 (sp^3) like hybridizations, which lower the core energy and remove the gap states.³⁴ Meanwhile, in the other structure, all the atoms

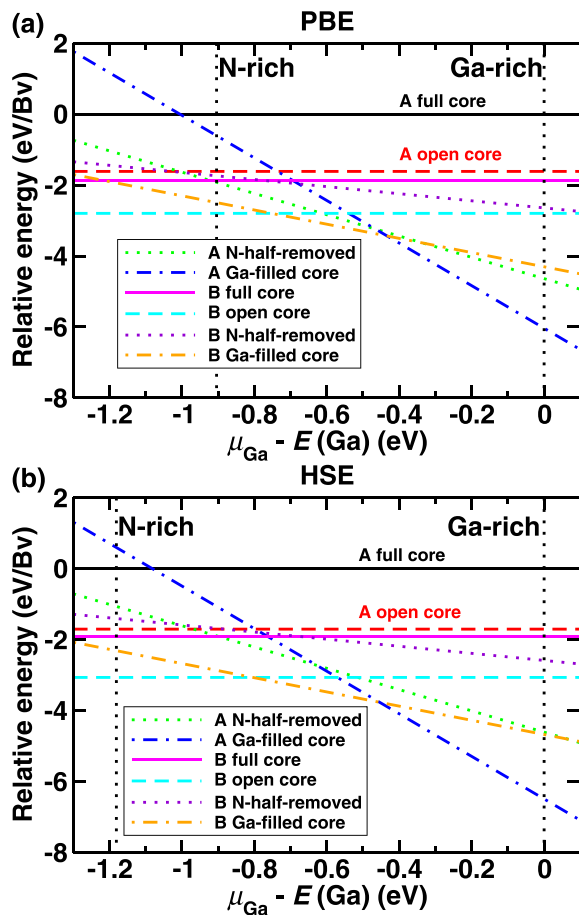


FIG. 3. The relative formation energies of various core structures obtained by (a) PBE and (b) HSE as a function of the difference of Ga chemical potential (μ_{Ga}) with regard to its value in elemental phase [$E(\text{Ga})$], whose maximum is 0 in Ga-rich limit and minimum is $\Delta H_f(\text{GaN})$ in N-rich limit. These two limits are plotted as vertical dotted bars in the figure.

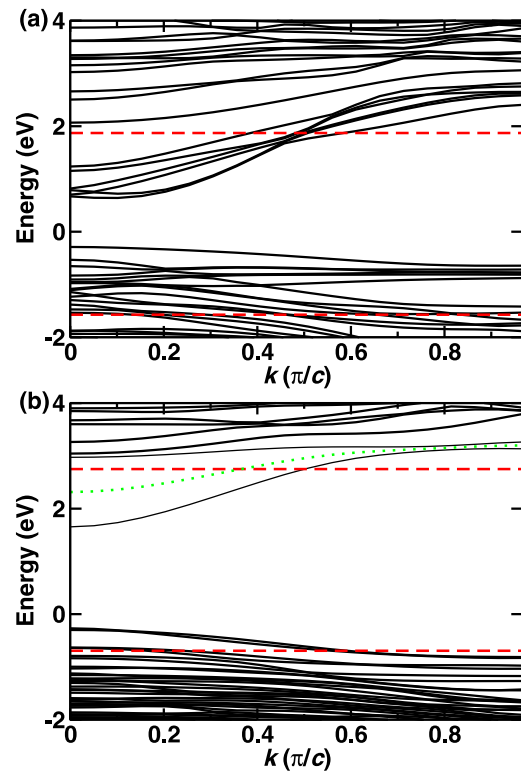


FIG. 4. The energy band structures along the [0001] direction calculated by HSE (a) for the screw "A" Ga-filled core and (b) for the screw "B" open core structure. Fermi energy is taken to be 0 eV. The red dashed lines correspond to the conduction band minimum (upper) and the valence band maximum (lower) of bulk GaN. The green dotted line in (b) represents the center of mass for the two artificially split states.

TABLE II. Bond lengths (minimum and maximum with average values in parenthesis) and bond angles (minimum and maximum with average values in parenthesis) of atoms located inside core region in the “B” open core configuration. The coordination numbers of each element are given in parentheses.

Atom	Bond lengths (Å)	Bond angles (°)
Hollow structure		
Ga (3)	1.83–1.93 (1.87)	106–128 (116)
N (3)	1.83–1.95 (1.88)	95–115 (107)
Ga (4)	1.88–2.01 (1.95)	95–123 (110)
N (4)	1.87–2.01 (1.95)	95–123 (109)
8/5-membered rings structure		
Ga (4)	1.89–2.43 (2.02)	95–143 (110)
N (4)	1.93–2.43 (2.03)	93–142 (109)

at 1' to 8' sites in Fig. 2 are four-fold coordinated (though Ga-N bonds between sites 1' and 8' and sites 4' and 5' are relatively weak with 2.43 Å bond distance), and no dangling bonds exist.

In Fig. 4(b), the energy band structure for “B” open core is shown. The band structure is calculated for the structure shown in Fig. 2, i.e., both hollow core and eight/five-membered rings core type structures are included. In this case, in contrast with “A” Ga-filled core structure, fewer states are introduced into the band gap region, whichever core structures are formed. We can notice that the lowest unoccupied state is split into two bands at the Brillouin zone center (Γ point, i.e., $k=0$) due to the artificial effect of overestimating the strain, which is caused by the dislocation dipole with small separation distance.³⁵ The center of mass for these two bands (~ 2.3 eV at Γ , marked by green dotted line) corresponds to the actual band position without the artificial effect. As a result, the introduced empty state is very shallow and the original band gap value is almost preserved. In the original study by Northrup,⁷ the most stable model in N-rich conditions is “A” N-half-removed core, which shows dangling bonds on Ga atoms. As a result, a couple of states are introduced in the band gap and some of them cross the Fermi level. Thus screw dislocation in GaN was predicted to be electrically active, regardless of sample growth conditions. On the other hand, in this work, “B” open core is obtained as the most stable structure in N-rich conditions, and it is expected to be electrically inactive, in agreement with experiments.

In summary, we obtained another structure as the most stable configuration for threading screw dislocation of wurtzite GaN in N-rich conditions by first-principles calculations using HSE hybrid functional. This structure is originated from “B” type screw dislocation with an open core configuration. Band structure calculation along the dislocation line for this stable structure shows that no deep states are introduced into the band gap and that the bulk band gap value is practically preserved. This suggests electrical inactivity of threading screw dislocations in GaN grown in N-rich conditions. This is consistent with recent experimental result obtained for GaN samples grown in N-rich conditions, which cannot be explained by the previously proposed theoretical

model. We believe that it is important to study the same dislocation core structure in order to understand the properties of a broader range of electronic materials that crystallize in wurtzite form.

The authors gratefully acknowledge financial support from the U. S. Army Research Laboratory through the Collaborative Research Alliance (CRA) for MultiScale multidisciplinary Modeling of Electronic materials (MSME). This work was performed using DoD HPCMP Open Research Systems computing resources.

- ¹N. G. Weimann, L. F. Eastman, D. Doppalapudi, H. M. Ng, and T. D. Moustakas, *J. Appl. Phys.* **83**, 3656 (1998).
- ²F. Bertazzi, M. Moresco, and E. Bellotti, *J. Appl. Phys.* **106**, 063718 (2009).
- ³T. Hino, S. Tomiya, T. Miyajima, K. Yanashima, S. Hashimoto, and M. Ikeda, *Appl. Phys. Lett.* **76**, 3421 (2000).
- ⁴J. W. P. Hsu, M. J. Manfra, S. N. G. Chu, C. H. Chen, L. N. Pfeiffer, and R. J. Molnar, *Appl. Phys. Lett.* **78**, 3980 (2001); J. W. P. Hsu, M. J. Manfra, R. J. Molnar, B. Heying, and J. S. Speck, *ibid.* **81**, 79 (2002).
- ⁵G. Koblmüller, F. Wu, T. Mates, J. S. Speck, S. Fernández-Garrido, and E. Calleja, *Appl. Phys. Lett.* **91**, 221905 (2007).
- ⁶J. J. M. Law, E. T. Yu, G. Koblmüller, F. Wu, and J. S. Speck, *Appl. Phys. Lett.* **96**, 102111 (2010).
- ⁷J. E. Northrup, *Phys. Rev. B* **66**, 045204 (2002).
- ⁸I. Belabbas, J. Chen, and G. Nouet, *Comput. Mater. Sci.* **51**, 206 (2012).
- ⁹H. Koizumi, Y. Kamimura, and T. Suzuki, *Philos. Mag. A* **80**, 609 (2000).
- ¹⁰L. Pizzagalli, P. Beauchamp, and J. Rabier, *Philos. Mag.* **83**, 1191 (2003).
- ¹¹C.-Z. Wang, J. Li, K.-M. Ho, and S. Yip, *Appl. Phys. Lett.* **89**, 051910 (2006).
- ¹²J. Elsner, R. Jones, P. K. Sitch, V. D. Porezag, M. Elstner, T. Frauenheim, M. I. Heggie, S. Öberg, and P. R. Briddon, *Phys. Rev. Lett.* **79**, 3672 (1997).
- ¹³J. E. Northrup, *Appl. Phys. Lett.* **78**, 2288 (2001).
- ¹⁴A. Béré and A. Serra, *Phys. Rev. B* **65**, 205323 (2002).
- ¹⁵Y.-N. Xu and W. Y. Ching, *Phys. Rev. B* **48**, 4335 (1993).
- ¹⁶B. Monemar, *Phys. Rev. B* **10**, 676 (1974).
- ¹⁷M. R. Ranade, F. Tessier, A. Navrotsky, V. J. Leppert, S. H. Risbud, F. J. DiSalvo, and C. M. Balkas, *J. Phys. Chem. B* **104**, 4060 (2000).
- ¹⁸H. Hahn and R. Juza, *Z. Anorg. Allg. Chem.* **244**, 111 (1940).
- ¹⁹A. Polian, M. Grimsditch, and I. Grzegory, *J. Appl. Phys.* **79**, 3343 (1996).
- ²⁰F. Oba, A. Togo, I. Tanaka, J. Paier, and G. Kresse, *Phys. Rev. B* **77**, 245202 (2008).
- ²¹A. Stroppa and G. Kresse, *Phys. Rev. B* **79**, 201201 (2009).
- ²²A. Janotti, J. B. Varley, P. Rinke, N. Umezawa, G. Kresse, and C. G. Van de Walle, *Phys. Rev. B* **81**, 085212 (2010).
- ²³D. O. Demchenko, I. C. Diallo, and M. A. Reshchikov, *Phys. Rev. Lett.* **110**, 087404 (2013).
- ²⁴J. Heyd, G. E. Scuseria, and M. Ernzerhof, *J. Chem. Phys.* **118**, 8207 (2003); **124**, 219906 (2006).
- ²⁵J. Paier, M. Marsman, K. Hummer, G. Kresse, I. C. Gerber, and J. G. Ángyán, *J. Chem. Phys.* **124**, 154709 (2006); **125**, 249901 (2006).
- ²⁶M. Jain, J. R. Chelikowsky, and S. G. Louie, *Phys. Rev. Lett.* **107**, 216806 (2011).
- ²⁷P. E. Blöchl, *Phys. Rev. B* **50**, 17953 (1994).
- ²⁸J. P. Perdew, K. Burke, and M. Ernzerhof, *Phys. Rev. Lett.* **77**, 3865 (1996).
- ²⁹G. Kresse and J. Furthmüller, *Phys. Rev. B* **54**, 11169 (1996); G. Kresse and D. Joubert, *ibid.* **59**, 1758 (1999).
- ³⁰J. R. K. Bigger, D. A. McInnes, A. P. Sutton, M. C. Payne, I. Stich, R. D. King-Smith, D. M. Bird, and L. J. Clarke, *Phys. Rev. Lett.* **69**, 2224 (1992).
- ³¹N. Lehto and S. Öberg, *Phys. Rev. Lett.* **80**, 5568 (1998).
- ³²A. Béré and A. Serra, *Philos. Mag.* **86**, 2159 (2006).
- ³³J. Hirth and J. Lothe, *Theory of Dislocations* (Wiley, 1982).
- ³⁴J. E. Northrup and J. Neugebauer, *Phys. Rev. B* **53**, R10477 (1996).
- ³⁵A. T. Blumenau, C. J. Fall, J. Elsner, R. Jones, M. I. Heggie, and T. Frauenheim, *Phys. Status Solidi C* **0**, 1684 (2003).